Received: 23 October 2017 | Accepted: 23 May 2018

DOI: 10.1002/jcp.26885

ORIGINAL RESEARCH ARTICLE

WILEY Journal of Cellular Physiology

CSDC2, a cold shock domain RNA-binding protein in decidualization

Griselda Vallejo[1] | Ana Cecilia Mestre-Citrinovitz[1] | Elke Winterhager[2] | Patricia Esther Saragüeta[1]

[1]Instituto de Biología y Medicina Experimental, IByME-Conicet, Buenos Aires, Argentina

[2]Department of Molecular Biology Medical School Essen University of Duisburg-Essen

Correspondence
Patricia Saragüeta, Instituto de Biología y Medicina Experimental, IByME-Conicet, Vuelta de Obligado 2490, C1428ADN Buenos Aires, Argentina.
Email:sarag@dna.uba.ar

Funding information
Consejo Nacional de Investigaciones Científicas y Técnicas, Grant/Award Number: PIP 2015 #682; Agencia Nacional de Promoción Científica y Tecnológica, Grant/Award Number: PICT 2015 #3426

RNA-binding proteins (RBPs) have been described for cancer cell progression and differentiation, although there is still much to learn about their mechanisms. Here, using in vivo decidualization as a model, we describe the role of RBP cold shock domain containing C2 (CSDC2) in the endometrium. *Csdc2* messenger RNA expression was differentially regulated depending on time and areas of decidua development, with the most variation in antimesometrium (AM) and, to a lesser degree, in the junctional zone (JZ). Immunohistochemistry of CSDC2 showed a preferentially cytoplasmic localization at AM and JZ, and nuclear localization in underneath myometrium and mesometrium (M). Cytoplasmic localization coincided with differentiated, DESMIN-marked areas, while nuclear localization coincides with proliferative zones. Uterine suppression of CSDC2 through intrauterine-injected-specific small interfering RNA (siRNA) led to abnormal decidualization in early pregnancy, with more extended antimesometrial area and with poor M development if compared with control siRNA-injected animals. These results suggest that CSDC2 could be a regulator during decidua development.

KEYWORDS
CSDC2, differentiation, endometrium, RNA-binding proteins

1 | INTRODUCTION

The uterus provides a unique and dynamic physiological model in which cellular proliferation, differentiation, and apoptosis occur in a temporal and cell-specific manner during pregnancy. Decidualization comprises a rapid remodeling of the uterine stromal compartment, resulting in a morphological and functional transformation. This complex shift in the cell fate builds the decidua, a specialized compact tissue responsible for successful implantation. Decidua plays a critical role to ensure proper maternal–fetal interactions and guide trophoblast invasion, placental orientation and development (Paria, Song, & Dey, 2001; Tranguch, Daikoku, Guo, Wang, & Dey, 2005). The transdifferentiation process of stromal cells is coordinated by the priming effect of steroid hormones estradiol and progesterone, and by the signaling interaction with the implanting blastocyst (Ramathal, Bagchi, Taylor, & Bagchi, 2010; Wang & Dey, 2006). Although numerous molecules of the signaling pathway necessary for decidual development have been identified, the hierarchical instructions that coordinate the ovarian hormone actions with the embryo-uterine dialogue are not well understood. For this reason finding master regulators for decidual regulation is crucial. We propose that cold shock domain containing C2 (CSDC2), a CSD protein involved in RNA binding during decidualization, could function as one of these decidual master regulators.

The decidua presents different morphological and functional areas: the antimesometrium (AM), is characterized by very compacted round cells and is the implantation site (IS) for the embryo; the mesometrium (M), a less compact area, is important for the development of vascularization and placenta. These two differentiated zones, AM and

Griselda Vallejo and Ana Cecilia Mestre-Citrinovitz are equal contributors.

M, are clearly separated by the junctional zone (JZ), so far considered undifferentiated, and also known as glycogenic area (O'Shea, Kleinfeld, & Morrow, 1983). The stromal area underneath the myometrium (UM) is also undifferentiated (Thienel, Chwalisz, & Winterhager, 2002).

Our previous results for in vitro decidualization using UIII rat normal endometrial stromal cells showed that, when cultured in the presence of 10% calf serum free of steroids, they acquired morphological features of decidual cells and expressed decidual markers (Vallejo et al., 2010). Genes involved in decidualization were identified using complementary DNA (cDNA) microarray. We found 322 annotated genes exhibiting significant differences in expression (>3-fold, fold discovery rate [FDR] > 0.005), of which 312 have not been previously related to decidualization. Out of these, *Csdc2* was the most upregulated during decidualization and was shown to be also regulated in uterine decidua during normal pregnancy (Vallejo et al., 2010).

CSDC2 is an RNA-binding protein (RBP), highly enriched in the rat brain, specifically enriched in some pyramidal neurons of the cerebral cortex and in the Purkinje cells of the cerebellum (Castiglia, Scaturro, Nastasi, Cestelli, & Di Liegro, 1996; Nastasi et al., 2000) and never described before in uterus. The protein structure contains a central CSD with both RNP1 and RNP2 motifs specialized in single-stranded RNA binding, and two putative double-stranded RNA-binding domains (PIP1 and PIP2; Nastasi et al., 1999). It binds with high specificity to the transcripts that encode H1° and H3.3 histone variants at the very end of their 3′ untranslated region, which encompasses the polyadenylation signal, possibly inhibiting polyadenylation and translation (Nastasi et al., 1999). It is suggested that CSDC2 downregulates the level of these histones during the rat brain development, facilitating the terminal differentiation of pyramidal neurons (Nastasi et al., 1999).

In this paper we study the role of RBP CSDC2 in in vivo decidualization.

2 | MATERIALS AND METHODS

2.1 | Animal care

Adult female Sprague Dawley rats were housed under defined conditions with a temperature of 22 ± 1°C, an atmospheric humidity of 55 ± 10%, and a 12 hr dark to 12 hr light cycle. They were provided with food and water ad libitum. All experimental procedures were performed according to NIH Guidelines for the Care and Use of Laboratory Animals, and approved by the Ethics and Research Committee from IBYME, Buenos Aires.

2.2 | Pregnancy

Female rats (280–330 g, 9–10 weeks old) were routinely cycled and the phase of the oestrous cycle was evaluated by vaginal smear. Rats at proestrus were matted overnight with males of proven fertility and the following morning the presence of cornificated cells and sperm was evaluated by vaginal smear. The day of sperm finding was designated as 0 day postcoitum (dpc).

2.3 | Tissue collection

The 0, 2, and 4 dpc uterine horns were removed and cut into pieces, which were frozen in liquid nitrogen for subsequent RNA isolation and western blot analysis. IS from 5, 6, 7, 8, 9, and 10 dpc uterine horns were dissected and frozen in liquid nitrogen for RNA isolation and western blot analysis, or fixed in 4% formalin for morphological and immunohistochemistry (IHC) analysis (Vallejo et al., 2011).

2.4 | Western blot analysis

Protein extracts were obtained from tissue samples by homogenization (Polytron PT-MR 300; Brinkmann Instruments, Westbury, NY) in radioimmunoprecipitation assay buffer (50 mM Tris–HCl, 150 mM NaCl, 1% v/v NP-40, 0.25% v/v Na-deoxycholate, 1 mM EDTA, 0.1% w/v sodium dodecyl sulfate) supplemented with 20 mM β glycerol phosphate, 25 mM sodium fluoride, 2 mM Na orthovanadate, 2 mM phenylmethylsulfonyl fluoride, 10.5 μM leupeptin, 7.3 μM pepstatin, 76.8 μM aprotinin (Sigma-Aldrich, St. Louis, MO). Protein concentration was determined by Nanodrop (NanoDrop 2000 Spectrophotometer; Thermo Fisher Scientific, Waltham, MA). Sodium dodecyl sulfate–polyacrylamide gel electrophoresis and immunoblot analysis were performed to detect CSDC2, extracellular signal-regulated kinase (ERK), and glyceraldehyde 3-phosphate dehydrogenase (GAPDH). The following antibodies were used: rabbit anti-CSDC2 (kindly gifted by Dr. Italia Di Liegro, Castiglia et al., 1996), rabbit monoclonal 14C10 anti-hGAPDH (Cell Signaling Technology, Beverly, MA); rabbit polyclonal C14 anti-rERK2 (Santa Cruz Biotechnology Inc., Santa Cruz, CA). A minimum of three blots from different rats was performed and the band intensities were measured with ImageQuant 3.3 program (Amersham Pharmacia Biotech, Arlington Heights, IL).

2.5 | Histology

IS were fixed in 4% formalin, dehydrated in a graded series of alcohol, and embedded in paraffin. Cross serial sections of 7 μm were deparaffinized, rehydrated in a graded series of alcohol, and stained with hematoxylin–eosin. Photographs were taken with a confocal microscope Nikon C1 Eclipse E800 (Nikon Instruments Inc., Melville, NY). The area of the different regions within the IS were quantified with Image J 1.43 software (Wayne Rasband, National Institute of Mental Health, Bethesda, MD) and delimited as shown in Figure 2. The contribution of the different tissue regions were calculated relative to the entire IS.

2.6 | CSDC2 in vivo depletion

For CSDC2 in vivo depletion, 5 dpc pregnant rats were placed under anesthesia with an intraperitoneal injection of ketamine (60 mg/kg)/xylazine (10 mg/kg). Ovaries were exposed by bilateral flank minor incisions and once the presence of IS was confirmed, 100 μl of minimum essential medium (Sigma-Aldrich) containing INTERFERin

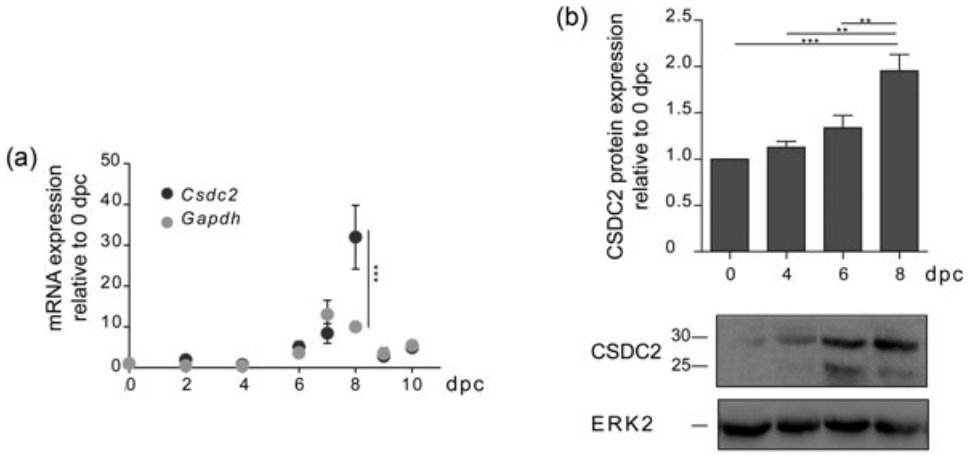

FIGURE 1 CSDC2 is induced during in vivo decidualization. Tissue from pregnant rat at different days postcoitum (dpc) or nonpregnant (0 dpc) was obtained from uterine horns (0, 2, and 4 dpc) and IS (6, 7, 8, 9, and 10 dpc) as indicated. (a) *Csdc2* and *Gapdh* mRNA expression of each sample was analyzed by qRT-PCR. Data represent *Csdc2* and *Gapdh* mRNA expression relative to nonpregnant content media ± *SEM* from two to three animals. One IS from each animal was analyzed. ***$p < 0.001$ statistical difference. (b) CSDC2 and ERK2 protein content was analyzed by western blot analysis and quantified. Upper graph shows CSDC2 protein content normalized by ERK2 protein content and relative to 0 dpc. Data represent CSDC2 positive signal or ERK total positive signal relative to 0 dpc content media ± *SEM* from three to four animals. One IS from each animal was analyzed. **$p < 0.01$ and ***$p < 0.001$ statistical difference. A representative western blot analysis of 50 μg of protein of each sample is shown. CSDC2, cold shock domain containing C2; ERK2, extracellular signal–regulated kinase; GADPH, glyceraldehyde 3-phosphate dehydrogenase; IS, implantation site; mRNA, messenger RNA; qRT-PCR, reverse transcription quantitative polymerase chain reaction; SEM, standard error of the media

transfection agent (Polyplus transfection, New York) and 10 nM CSDC2 siRNA (PIPPIN siRNA sc-76146; Santa Cruz Biotechnology Inc.) were intrauterine injected after the oviduct at the beginning of the uterine horn. The contralateral horn was intrauterine injected with 100 nM *Csdc2* siRNA. Control animal were intrauterine injected with 10 nM nontargeting control siRNA pool (Dharmacon Research, Inc., Lafayette, CO) in one horn and 100 nM nontargeting control siRNA pool in the contralateral horn pool, unless in the case of Figure 5d when replicates were increased with quantified areas of IS from animals injected with 100 nM nontargeting control siRNA in one horn and 100 nM CSDC2 siRNA in the contralateral horn. The muscle was sutured, and the skin was closed with contact adhesive. After 2 days animals were euthanized under carbon dioxide chamber followed by cervical dislocation.

2.7 | IHC

For immunostaining paraffin sections (7 μm) were deparaffinized and rehydrated in a graded series of alcohols. After rinsing with phosphate-buffered saline (PBS; 1 × 5 min), the endogenous peroxidase was blocked. The sections were boiled for 20 min in citrate buffer and left at room temperature (RT) for 40 min before blocking with 2% bovine serum albumin (BSA; Sigma-Aldrich). Controls were performed omitting the primary antibody and incubated with the antibody solution (0.5% BSA-PBS). The sections were incubated overnight at 4°C with the primary antibodies, rinsed in PBS (3 × 5 min), incubated with a secondary biotinylated antibody (30 min RT), and after that with streptavidin–peroxidase complex (Millipore, Billerica, NA) during 30 min. Staining was visualized with 3.3 diaminobenzidine (DAB; Sigma-Aldrich). The following antibodies were used: rabbit polyclonal anti-CSDC2 AV40768 (RRID: AB_1847265; Sigma-Aldrich), rabbit polyclonal anti-KI67 Ab15580 (RRID:AB_443209; Abcam, Cambridge, MA), mouse monoclonal anti-human Desmin, clone D33 (RRID:AB_2335684; Dako, Glostrup, Denmark), rabbit monoclonal D13.14.4E anti-hERK1–2 phosphorylated at Thr202/Tyr204 (RRID:AB_2315112; Cell Signaling Technology, Beverly, MA), rabbit polyclonal H-190 anti-hPR (Santa Cruz Biotechnology, Inc.), polyclonal goat anti-mouse immunoglobulins/biotinylated (RRID:AB_2687905), and polyclonal goat anti-rabbit immunoglobulins/biotinylated (RRID:AB_2313609; Dako).

2.8 | Laser capture collection and RNA isolation

Microdissection from nonpregnant (0 dpc), complete 8 dpc implantations sites, and different regions within the 8 dpc IS were performed with ArcturusXT Laser Capture Microdissection System (Thermo Fisher Scientific) coupled with an Eclipse Ti-E inverted microscope (Nikon Instruments, Inc., Melville, NY). Briefly, frozen IS were sectioned with a cryostat (Cryotome E; Thermo Fisher Scientific) in consecutive 30 μm sections for subsequent tissue microdissection and RNA isolation. The zone of interest was identified under 2× objective and delimited under 20× objective, captured with a IR laser, cut with a UV laser and collected in a cap. RNA was isolated with PicoPure RNA Isolation kit according to manufacturer instructions (Thermo Fisher Scientific).

2.9 | Reverse transcription quantitative polymerase chain reaction (RT-qPCR)

RNA extracts from Figure 1a were obtained from tissue samples by homogenization (Polytron PT-MR 300; Brinkmann Instruments, Westbury, NY) in guanidinium thiocyanate solution and total RNA isolation was performed according to guanidinium thiocyanate–phenol–chloroform extraction single-step method (Chomczynski & Sacchi, 1987). Subsequently, cDNA was synthesized as previously described (Vallejo, Ballare, Baranao, Beato, & Saragueta, 2005). cDNA from laser-captured samples was synthesized with qScript-cDNA synthesis kit (Quanta Biosciences, Beverly, MA) according to manufacturer's instructions.

Real-time PCR were performed with 5 × HOT FIREPol EvaGreen qPCR Mix Plus (Solis BioDyne, Tartu, Estonia) using the ABI PRISM 7500 (Applied Biosystems, Foster City, CA; Thermo Fisher Scientific, Waltham, MA; PCR detection systems, Waltham, MA). *Gapdh* and 18S were used as RNA template control. The identity of the PCR products was verified by melting curve analyses and agarose gel electrophoresis. Fluorescent values were measured at 520 nm. Crossing threshold (C_t) values were calculated with 7500 System Software Sequence Detection System 1.3 (Applied Biosystems) or Bio-Rad CFX Manager 3.0 (Bio-Rad Laboratories), respectively. Relative quantification was carried out according to Delta CT method (Vicent et al., 2013). cDNA primers are available in Supporting Information Table 1.

2.10 | Statistical analysis

Analysis of variance was used for statistical testing, followed by Tukey Multiple Comparison Test in Figures 1, 2c,d. The *t* test was performed in

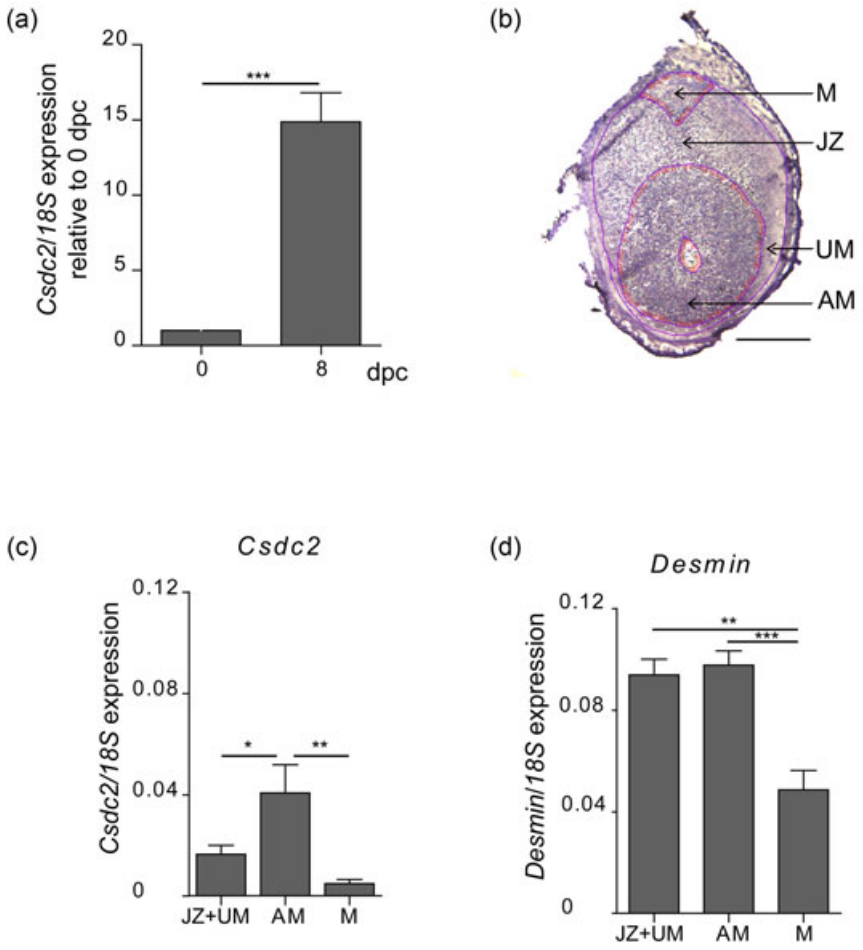

FIGURE 2 *Csdc2* mRNA increases differentially at the AM and JZ decidua. (a) RNA from frozen tissue of 8 dpc IS and nonpregnant rats (0 dpc) uterine horns was obtained with laser capture technology and analyzed by qRT-PCR. Data represent *Csdc2* mRNA normalized by 18S RNA expression and relative to 0 dpc media±*SEM* from qPCR replicates from one 0 dpc and one 8 dpc animal. One tissue sample from each animal was analyzed. ***$p < 0.001$ statistical difference. (b) Laser capture analysis of 8 dpc IS morphology. Laser capture and RNA extraction of different decidual areas were highlighted in a 20 μm frozen section from an 8 dpc IS stained with HistoGene. Scale bar = 1000 μm. (c) *Csdc2* mRNA and 18S RNA were analyzed by qRT-PCR. Data represent *Csdc2* mRNA relative to 18S RNA content media±*SEM* from two animals. Samples from each animal correspond to captures from two IS and qPCR was performed in triplicates. *$p < 0.05$, and **$p < 0.01$ statistical difference. (d) Desmin mRNA and 18S RNA were analyzed by qRT-PCR. Data represent *desmin* mRNA relative to 18S RNA content media±*SEM* from two animals. Samples from each animal correspond to captures from two IS and qPCR was performed in triplicates. **$p < 0.01$ and ***$p < 0.001$ statistical difference. AM, antimesometrium; dpc, day postcoitum; IS, implantation site; JZ, junctional zone; mRNA, messenger RNA; M, mesometrium; qRT-PCR, reverse transcription quantitative polymerase chain reaction; UM, underneath myometrium [Color figure can be viewed at wileyonlinelibrary.com]

Figure 2a. Differences were considered significant if $p < 0.05$. Statistical analysis was carried out with GraphPad Prim 4.0 (RRID:SCR_002798; GraphPad Software Inc., La Jolla, CA). Differential region areas in Figure 5d were analyzed by descriptive statistics with Xlstat 2016.3 software (RRID:SCR_016137; Addinsoft, New York, NY). A notched box-plot (95% confidence interval [CI]) was performed. It was considered that medians differ with a 95% CI when the boxes' notches do not overlap.

3 | RESULTS

3.1 | CSDC2 is regulated during decidualization

Previous works showed that *Csdc2* was the most upregulated mRNA during in vitro decidualization as well as upregulated in uterine decidua during normal pregnancy (Vallejo et al., 2010). We extended decidual expression during the kinetics of rat pregnancy and found that it increased at 7 dpc, reaching its maximum mRNA expression at 8 dpc (Figure 1a). The *Csdc2* mRNA expression correlated with CSDC2 protein increment at 8 dpc (Figure 1b).

To localize the specific decidual area for *Csdc2* expression we performed a laser capture extraction for slices from 8 dpc IS (Figure 2). Total RNA was extracted and *Csdc2* expression of 0 dpc uterus and 8 dpc IS was quantified by qRT-PCR (Figure 2a), confirming *Csdc2* increment at 8 dpc shown in Figure 1 and done with the specific laser capture extraction protocol. HistoGene stained 8 dpc IS show different decidual highlighted areas: AM, M, and JZ plus the undifferentiated underneath myometrium (UM) zone (Figure 2b). A collection of 11–15 total fragments—taken from two IS from each

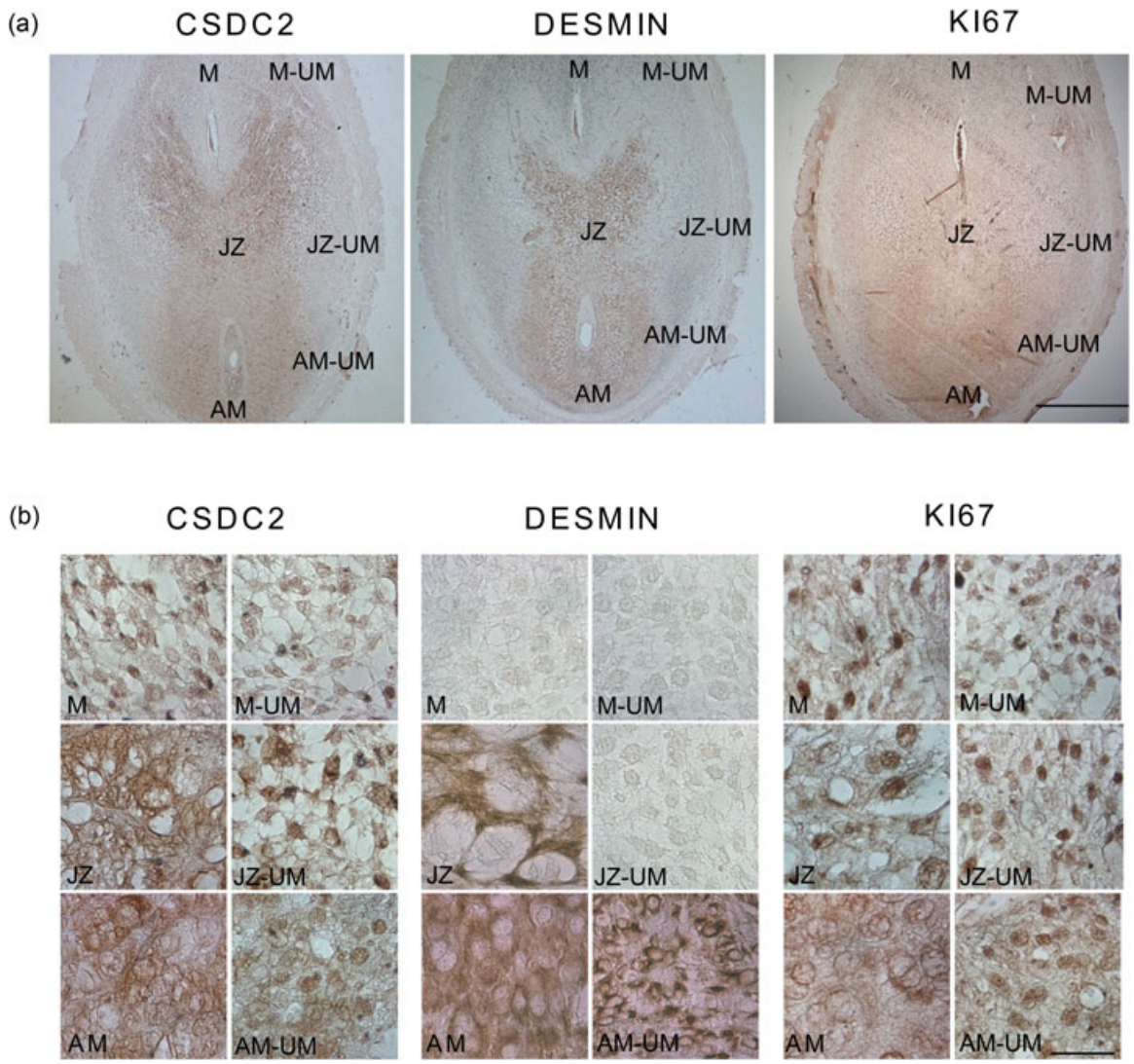

FIGURE 3 CSDC2 and DESMIN protein expression are associated in differentiated areas. Localization of CSDC2, DESMIN, and KI67 was analyzed by IHC in 8 dpc IS. Two animals, one implantation site from each animal, were analyzed for CSDC2 and DESMIN expression. One implantation site from one animal was analyzed for KI67 expression. IHC was performed at least twice in different slices from each implantation site. (a) Figure shows a representative 8 dpc IS CSDC2, DESMIN, and KI67 immunostaining. Scale bar = 1000 μm. (b) Details of CSDC2, DESMIN, and KI67 immunostaining at central areas of M, JZ, and AM (M, JZ, AM) and at the border of M, JZ, and AM (M-UM, JZ-UM, AM-UM). Scale bar = 25 μm. AM, antimesometrium; CSDC2, cold shock domain containing C2; dpc, day postcoitum; IHC, immunohistochemistry; IS, implantation site; JZ, junctional zone; M, mesometrium; UM, underneath myometrium [Color figure can be viewed at wileyonlinelibrary.com]

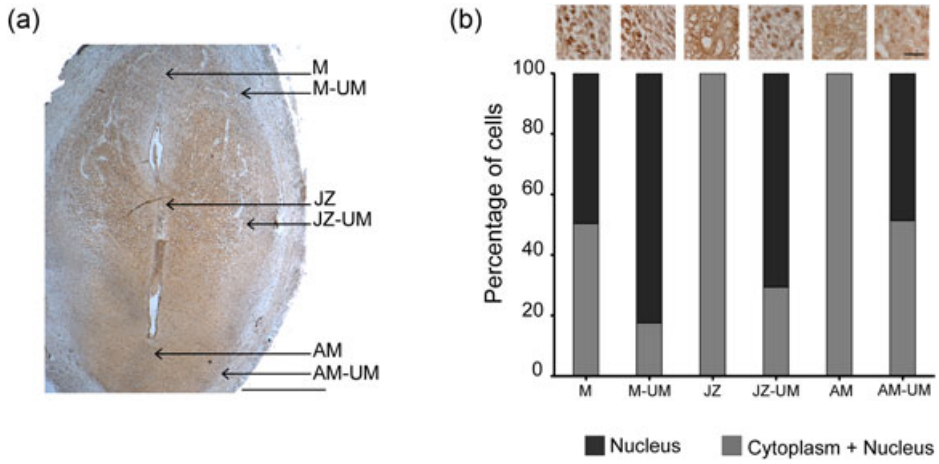

FIGURE 4 CSDC2 protein is cytoplasmic in differentiated decidual areas and nuclear in proliferative ones. Localization of CSDC2 was analyzed by IHC in 8 dpc IS. Two animals, one implantation site from each animal, were analyzed for CSDC2 expression. IHC was performed at 2–4 times in different slices from each implantation site. (a) Figure shows a representative 8 dpc IS CSDC2 immunostaining. Scale bar = 1000 μm. (b) Details of IS CSDC2 immunostaining at central zones of M, JZ, and AM (M, JZ, AM) and at the border of M, JZ, and AM (M-UM, JZ-UM, AM-UM). Bar graph shows the percentage of cells showing positive CSDC2 immunostaining at the nucleus (nucleus, black bar) or at the cytoplasm and nucleus (cytoplasm + nucleus, gray bar). Scale bar = 25 μm. AM, antimesometrium; CSDC2, cold shock domain containing C2; dpc, day postcoitum; IHC, immunohistochemistry; IS, implantation site; JZ, junctional zone; M, mesometrium; UM, underneath myometrium [Color figure can be viewed at wileyonlinelibrary.com]

animal—of these three areas were subjected to RNA extraction and amplified by qRT-PCR. The content of *Csdc2* mRNA was significantly higher in AM, followed by its expression in JZ + UM and barely noticeable in the M (Figure 2c). These results indicate a differentially regulated *Csdc2* mRNA expression depending on its morphological localization.

To associate morphological areas to differentiation qRT-PCR for *desmin* was performed in the same samples (Figure 2d). The pattern of *desmin* mRNA was similar to *Csdc2*, with no difference in *desmin* mRNA between the JZ and AM. This result suggests a differentiated state for the JZ.

3.2 | Nuclear CSDC2 is connected to proliferation and cytoplasmic CSDC2 to terminal differentiation

To confirm differential states of differentiation suggested by mRNA expression IHQ for DESMIN, pERK—a JZ specific marker according to our previous results (Vallejo et al., 2011) and Progesterone Receptor (PR)—a nuclear transcription factor of antimesometrial, JZ and mesometrial cells from the endometrium (Vallejo et al., 2011) was performed in 8 dpc IS (Figure 3 and Supporting Information Figure 1). IHC negative controls omitting the first antibody were performed (Supporting Information Figure 2). The AM, a terminally differentiated area, presented a DESMIN positive signal and so did the JZ, while the M was negative for DESMIN (Figure 3b, middle panel). These results suggest that the JZ is not a simple intersection area and lead us to think that it should be regarded as a differentiated area with a specific function, different from the AM and the M, similar to the AM and not to the M.

To associate CSDC2 with the differentiation state, IHC of CSDC2 was performed (Figure 3, left panel). A strong correlation of DESMIN and CSDC2 localization suggests that both proteins are a common feature of a differentiated phenotype of the AM and the JZ. This coincides with *desmin* mRNA expression determined in the AM and the JZ described above (Figure 2d).

To explore the localization of CSDC2 with the proliferative capacity of cells containing it, KI67 IHC was performed. Figure 3 (right panel) shows that the M and the border of the JZ are positive for this proliferative marker, while the AM area is negative. Nuclear CSDC2 correlates with positive KI67 nucleus of AM cells in the UM, of M and of JZ cells. Then nuclear CSDC2 colocalizes with proliferative decidual cells.

CSDC2 protein localization analyzed by IHC (Figure 4) shows a positive signal in all decidual areas with different density and subcellular localization, cytoplasmic and nuclear localization in the AM, cytoplasmic and strong perinuclear localization in JZ, strong nuclear localization in the UM area, to a lesser degree in the cytoplasm and, with a strong signal (but not in all cells), in the nucleus of mesometrial cells (Figure 4a). Considering percentages of cells with cytoplasmic + nuclear and nuclear subcellular localization, the AM and the JZ are the decidual areas with the highest cytoplasmic + nuclear subcellular localization, with the protein preferentially in the cytoplasm, while this percentage is the smallest for the M, with a preferentially nuclear localization (Figure 4b). The JZ showed two different patterns: A cytoplasmic one in the center of the IS and a nuclear one as it gets closer to the UM area. This latter result suggests that the differentiation process is clearer in the JZ. Taken together, Figures 3 and 4 prove that nuclear CSDC2 is connected to proliferation and cytoplasmic CSDC2 to terminal differentiation in the decidua and that CSDC2 could regulate differentiation during decidua development.

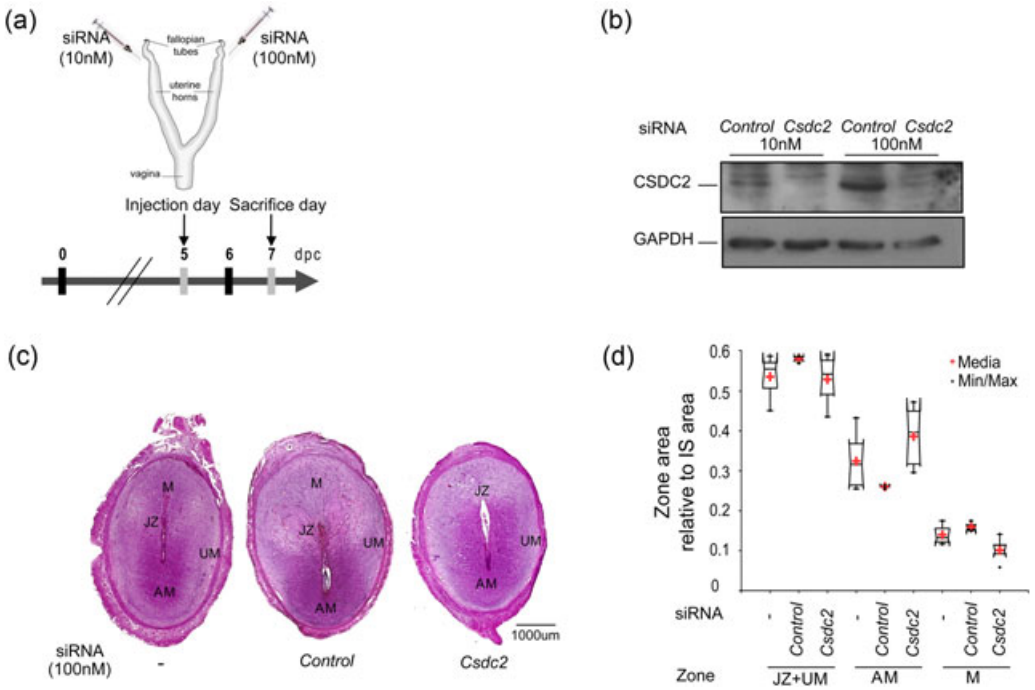

FIGURE 5 *Csdc2* depletion reduces M development. (a) The scheme represents *Csdc2* depletion protocol. *Csdc2* siRNA at 10 and 100 nM, and control siRNA were injected in the uteri of 5 dpc pregnant rats and killed at 7 dpc. (b) A representative western blot analysis for CSDC2 and GADPH content from control and *Csdc2* siRNA 7 dpc IS is shown. (c) Hematoxylin–eosin stained 7 μm paraffin sections from 7 dpc IS of animals not injected (–) and injected with 100 nM control siRNA (control) and 100 nM *Csdc2* siRNA (*Csdc2*) shows a representative IS section from three animals. Scale bar = 1000 μm. (d) Notched box-plot shows quantification of IS, JZ + UM, AM, and M areas from untreated animals and animals treated with 100 nM control siRNA and 100 nM *Csdc2* siRNA. Median, 75th and 25th percentile from three animals for each treatment are shown. Three IS slices were quantified from each animal. Red cross = media, black diamond = min–max values. AM, antimesometrium; CSDC2, cold shock domain containing C2; dpc, day postcoitum; GADPH, glyceraldehyde 3-phosphate dehydrogenase; IS, implantation site; JZ, junctional zone; M, mesometrium; siRNA, small interfering RNA; UM, underneath myometrium [Color figure can be viewed at wileyonlinelibrary.com]

3.3 | Uterine suppression of CSDC2 leads to abnormal decidualization in early pregnancy

To explore the role of CSDC2 during early decidualization, CSDC2 was depleted using specific siRNA (Figure 5). The 10 nM siRNA against *Csdc2* was injected in one uterine horn and 100 nM *CsdC2* siRNA in the contralateral horn of 5 dpc pregnant rats after implantation, which in rats occurs at 4.5 dpc, to discriminate between decidualization and embryo implantation. Control animals were intrauterine injected with 10 nM nontargeting control siRNA in one horn and 100 nM nontargeting control siRNA in the contralateral horn. The animals were killed at 7 dpc and IS morphology was analyzed (Figure 5a, protocol). Depletion of CSDC2 was corroborated by western blot analysis (Figure 5b). Site-specific expression of CSDC2 was examined by IHC in the same CSDC2-depleted samples (Supporting Information Figure 3). The results showed that, indeed, CSDC2 was specifically reduced in the AM of CSDC2-specific siRNA-treated IS.

The morphology was analyzed by quantification of IS, JZ, and UM (JZ + UM), AM, and M areas of eosin–hematoxylin stained paraffin-embedded nontreated IS and treated with control siRNA and siRNA against *Csdc2* (Figure 5c). CSDC2 depletion was concomitant with a significant reduction in mesometrial decidua and with an increment in the antimesometrial area in CSDC2 siRNA-treated animals compared with the same areas in control siRNA-treated and untreated animals (Figure 5d). In summary, our results suggest that CSDC2 is involved in the antimesometrial and JZ late differentiation and in proliferation of junctional UM and M, with a consequent adequate balance between all decidual areas (Figure 6).

4 | DISCUSSION

RBPs have been described in cancer progression and differentiation because of their role in translation (Wurth & Gebauer, 2015). The presence and roles of RBP in differentiation, particularly in decidualization, remains unexplored to date. Decidualization is a process with active protein synthesis (Heald & O'Grady, 1970), which implies active RNA regulation and processing. RBPs orchestrate transcript fate and function (Szostak & Gebauer, 2013). Alterations in posttranscriptional events and RBP-mediated control in decidualization have never been studied.

Csdc2 mRNA is the most upregulated after decidual cell differentiation (Vallejo et al., 2010). Here we describe for the first time that CSDC2, an RBP, is one of the proteins that increases their amount during pregnancy. The spatiotemporal regulation of CSDC2

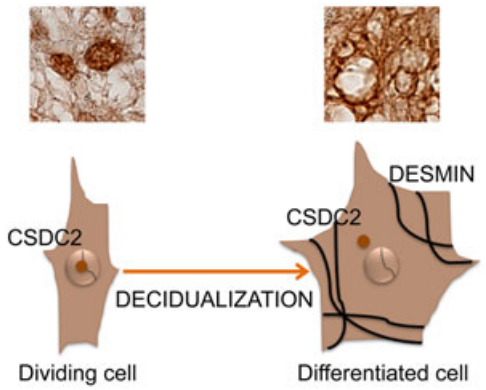

FIGURE 6 CSDC2 during decidualization. The scheme depicts subcellular CSDC2 localization during decidualization and its association with proliferative and differentiated states in endometrial cells. DESMIN is a marker of differentiated states of AM and JZ. Upper insets show CSDC2 immunofluorescence details of JZ in proliferative and differentiated states. AM, antimesometrium; CSDC2, cold shock domain containing C2; JZ, junctional zone [Color figure can be viewed at wileyonlinelibrary.com]

during decidualization in normal rat pregnancy has been explored. The highest *Csdc2* upregulation at 8 dpc decidua was associated to the AM and JZ, differentiated parts of decidua. Localization of CSDC2 in differentiated areas occurs at the cytoplasm of the cells, while this protein is mainly nuclear in areas under proliferation, as has been seen in the M and the most external JZ.

Contrary to general belief, our results show that the JZ is differentiated, although not in the same way as the AM and the M. It could be said that it is a combination of cells with desmin production in the areas near the embryo and of cells under proliferation as they approach the UM.

The decrease of CSDC2 shown at day 7 impairs mesometrial development. At 7 dpc, supposing the pregnancy has developed normally, the AM area could constitute the secondary decidual zone. The imbalance in mesometrial and antimesometrial development produced by depletion of CSDC2 could be a consequence of a negative regulation over the M and/or a positive deregulation over the antimesometrial decidualization (both proliferation and differentiation), or of a negative effect on regression events of the AM and the JZ. This case—JZ differentiation—might be working as an inhibition to the AM, giving rise to mesometrial normal development. Although M areas were affected by depletion of CSDC2 by siRNA after 5 dpc it would be interesting to develop a model of implantation without any CSDC2 at all, by injection before this process begins.

The effect of CSDC2 over the AM and the JZ could be a consequence of mRNA translational regulation, which may imply a movement of CSDC2 from nucleus (in proliferative cells) to cytoplasm (in differentiated cells). The effect of CSDC2 over proliferative cells could be a consequence of mRNA splicing or other nuclear gene regulation processes.

We speculate that posttranscriptional modifications of CSDC2, that is phosphorylation, could be a differential spatial change that could modify protein cytoplasmic or nuclear function. We explored the influence of pERK on CSDC2 with negative results; then other kinases need to be explored in coming studies.

It is yet to be found out which are the mRNA targets of CSDC2 in the AM and the JZ and which is the role of CSDC2 in the nucleus of proliferative decidual cells.

ACKNOWLEDGMENTS

The authors thank Pablo Pomata for laser dissection and microscopy support, Inti Tarifa-Rieschle for technical assistance, Italia Di Liegro, Francisco Pisciottano and Alejandro La Greca for helpful discussions and suggestions, Marta Merajver for critical reading of the manuscript, Gabriela Diessler for her kindly support, Fundación Williams and Fundación René Barón for having generously contributed with essential institutional equipment. This study was supported by grants to P. S. (contract grant sponsor: Agencia Nacional de Promoción Científica y Tecnológica Argentina, contract grant number: PICT 2015 #3426 and contract grant sponsor: Consejo Nacional de Investigaciones Científicas y Técnicas, contract grant number: PIP 2015 #682). The funders had no role in study design, data collection and analysis, decision to publish, or preparation of the manuscript.

ORCID

Patricia Saragüeta http://orcid.org/0000-0001-8222-9690

REFERENCES

Castiglia, D., Scaturro, M., Nastasi, T., Cestelli, A., & Di Liegro, I. (1996). PIPPin, a putative RNA-binding protein specifically expressed in the rat brain. *Biochemical and Biophysical Research Communications*, *218*(1), 390–394.

Chomczynski, P., & Sacchi, N. (1987). Single-step method of RNA isolation by acid guanidinium thiocyanate-phenolchloroform extraction. *Analytical Biochemistry*, *162*, 156–159.

Heald, P. J., & O'Grady, J. E. (1970). The uptake of [3H] uridine into the nucleic acids of rat uterus during early pregnancy. *Biochemical Journal*, *117*(1), 65–71.

Nastasi, T., Muzi, P., Beccari, S., Bellafiore, M., Dolo, V., Bologna, M., … Di Liegro, I. (2000). Specific neurons of brain cortex and cerebellum are PIPPin positive. *Neuroreport*, *11*(10), 2233–2236.

Nastasi, T., Scaturro, M., Bellafiore, M., Raimondi, L., Beccari, S., Cestelli, A., & Di Liegro, I. (1999). PIPPin is a brain-specific protein that contains a cold-shock domain and binds specifically to H1 degrees and H3.3 mRNAs. *Journal of Biological Chemistry*, *274*(34), 24087–24093.

O'Shea, J. D., Kleinfeld, R. G., & Morrow, H. A. (1983). Ultrastructure of decidualization in the pseudopregnant rat. *The American Journal of Anatomy*, *166*(3), 271–298.

Paria, B. C., Song, H., & Dey, S. K. (2001). Implantation: Molecular basis of embryo-uterine dialogue. *International Journal of Developmental Biology*, *45*(3), 597–605.

Ramathal, C., Bagchi, I., Taylor, R., & Bagchi, M. (2010). Endometrial decidualization: Of mice and men. *Seminars in Reproductive Medicine*, *28*(1), 17–26.

Szostak, E., & Gebauer, F. (2013). Translational control by 3′-UTR-binding proteins. *Briefings in Functional Genomics*, *12*(1), 58–65.

Thienel, T., Chwalisz, K., & Winterhager, E. Expression of MAPkinases (Erk1/2) during decidualization in the rat: Regulation by progesterone and nitric oxide 2002. *Molecular Human Reproduction*, *8*(5), 465–474.

Tranguch, S., Daikoku, T., Guo, Y., Wang, H., & Dey, S. K. (2005). Molecular complexity in establishing uterine receptivity and implantation. *Cellular and Molecular Life Sciences*, *62*(17), 1964–1973.

Vallejo, G., Ballaré, C., Lino barañao, J., Beato, M., & Saragüeta, P. (2005). Progestin activation of nongenomic pathways via cross talk of progesterone receptor with estrogen receptor beta induces proliferation of endometrial stromal cells. *Molecular Endocrinology*, *19*, 3023–3037.

Vallejo, G., Maschi, D., Mestre-Citrinovitz, A. C., Aiba, K., Maronna, R., Yohai, V., … Saragüeta, P. (2010). Changes in global gene expression during in vitro decidualization of rat endometrial stromal cells. *Journal of Cellular Physiology*, *222*(1), 127–137.

Vallejo, G., Mestre-Citrinovitz, A. C., Mönckedieck, V., Grümmer, R., Winterhager, E., & Saragüeta, P. (2011). Ovarian steroid receptors and activated MAPK in the regional decidualization in rats. *Biology of Reproduction*, *84*(5), 1063–1071.

Vicent, G. P., Nacht, A. S., Zaurin, R., Font-Mateu, J., Soronellas, D., Le Dily, F., … Beato, M. (2013). Unliganded progesterone receptor-mediated targeting of an RNA-containing repressive complex silences a subset of hormone-inducible genes. *Genes and Development*, *27*(10), 1179–1197.

Wang, H., & Dey, S. K. (2006). Roadmap to embryo implantation: Clues from mouse models. *Nature Reviews Genetics*, *7*(3), 185–199.

Wurth, L., & Gebauer, F. (2015). RNA-binding proteins, multifaceted translational regulators in cancer. *Biochimica et Biophysica Acta*, *1849*(7), 881–886.

SUPPORTING INFORMATION

Additional supporting information may be found online in the Supporting Information section at the end of the article.

How to cite this article: Vallejo G, Mestre-Citrinovitz AC, Winterhager E, Saragüeta PE. CSDC2, a cold shock domain RNA-binding protein in decidualization. *J Cell Physiol*. 2019;234:740–748. https://doi.org/10.1002/jcp.26885